



OPEN ACCESS

EDITED BY
Christopher Rensing,
Fujian Agriculture and Forestry
University, China

REVIEWED BY
Anukool Vaishnav,
Agroscope, Switzerland
Fenglong Wang,
Tobacco Research Institute (CAAS),
China

*CORRESPONDENCE
Zhiping Wang
wangzp@syau.edu.cn
Yuanhua Wu
wuyh09@syau.edu.cn

SPECIALTY SECTION
This article was submitted to
Microbiotechnology,
a section of the journal
Frontiers in Microbiology

RECEIVED 21 December 2021

ACCEPTED 05 July 2022

PUBLISHED 28 July 2022

CITATION
Liu H, Jiang J, An M, Li B, Xie Y, Xu C,
Jiang L, Yan F, Wang Z and Wu Y (2022)
Bacillus velezensis SYL-3 suppresses
Alternaria alternata and tobacco
mosaic virus infecting *Nicotiana
tabacum* by regulating the
phyllosphere microbial community.
Front. Microbiol. 13:840318.
doi: 10.3389/fmicb.2022.840318

COPYRIGHT
© 2022 Liu, Jiang, An, Li, Xie, Xu, Jiang,
Yan, Wang and Wu. This is an
open-access article distributed under
the terms of the [Creative Commons
Attribution License \(CC BY\)](https://creativecommons.org/licenses/by/4.0/). The use,
distribution or reproduction in other
forums is permitted, provided the
original author(s) and the copyright
owner(s) are credited and that the
original publication in this journal is
cited, in accordance with accepted
academic practice. No use, distribution
or reproduction is permitted which
does not comply with these terms.

Bacillus velezensis SYL-3 suppresses *Alternaria alternata* and tobacco mosaic virus infecting *Nicotiana tabacum* by regulating the phyllosphere microbial community

He Liu¹, Jun Jiang¹, Mengnan An¹, Bin Li², Yunbo Xie²,
Chuantao Xu^{1,3}, Lianqiang Jiang⁴, Fangfang Yan⁵,
Zhiping Wang^{1*} and Yuanhua Wu^{1*}

¹Liaoning Key Laboratory of Plant Pathology, College of Plant Protection, Shenyang Agricultural University, Shenyang, China, ²Sichuan Province Tobacco Company, Chengdu, China, ³Sichuan Province Tobacco Company, Luzhou, China, ⁴Sichuan Province Tobacco Company, Xichang, China, ⁵Sichuan Province Tobacco Company, Panzhihua, China

The occurrence of plant diseases is closely associated with the imbalance of plant tissue microecological environment. The regulation of the phyllosphere microbial communities has become a new and alternative approach to the biological control of foliar diseases. In this study, *Bacillus velezensis* SYL-3 isolated from Luzhou exhibited an effective inhibitory effect against *Alternaria alternata* and tobacco mosaic virus (TMV). The analysis of phyllosphere microbiome by PacBio sequencing indicated that SYL-3 treatment significantly altered fungal and bacterial communities on the leaves of *Nicotiana tabacum* plants and reduced the disease index caused by *A. alternata* and TMV. Specifically, the abundance of *P. seudomo*, *Sphingomonas*, *Massilia*, and *Cladosporium* in the SYL-3 treatment group increased by 19.00, 9.49, 3.34, and 12.29%, respectively, while the abundances of *Pantoea*, *Enterobacter*, *Sampaiozyma*, and *Rachicladosprium* were reduced. Moreover, the abundance of beneficial bacteria, such as *Pseudomonas* and *Sphingomonas*, was negatively correlated with the disease indexes of *A. alternata* and TMV. The PICRUSt data also predicted the composition of functional genes, with significant differences being apparent between SYL-3 and the control treatment group. Further functional analysis of the microbiome also showed that SYL-3 may induce host disease resistance by motivating host defense-related pathways. These results collectively indicate that SYL-3 may suppress disease progression caused by *A. alternata* or TMV by improving the microbial community composition on tobacco leaves.

KEYWORDS

Bacillus velezensis SYL-3, *Alternaria alternata*, tobacco mosaic virus, *Nicotiana tabacum*, phyllosphere microbial community

Introduction

Microorganisms are ubiquitous in nature and influence everyday life in various harmful as well as beneficial ways (Morelli and Pellegrino, 2021). Currently, biological control using microorganisms and their metabolites has been used as a potentially effective, sustainable, and alternative method (Zhang N. et al., 2017). The microorganisms such as the genera *Bacillus*, *Pseudomonas*, *Trichoderma*, as well as *Streptomyces* have been reported to effectively inhibit the occurrence and pathogenesis of plant diseases caused by various pathogenic fungi, bacteria, and viruses (Ashrafi et al., 2021; Gao et al., 2021; Jiang et al., 2021; Sánchez-Montesinos et al., 2021). The major *Bacillus* spp. that has been applied in biological control are *B. subtilis*, *B. megaterium*, *B. amyloliquefaciens*, and *B. velezensis* (Wang Y. et al., 2020; Zeng et al., 2021). *Bacillus* is a well-known producer of a wide array of antagonistic compounds with different structures, namely, peptides, lipopeptides, bacteriocins, and polyketide compounds (Fira et al., 2018). For instance, the *B. amyloliquefaciens* PPL strain can suppress the infection of cucumber mosaic virus as well as upregulate plant defense-related genes by producing fengycin (Kang et al., 2021). *B. velezensis* AR1 has been reported to resist *Alternaria* leaf spots caused by *Alternaria sesami* and improve plant physiological traits by inducing resistance in the host (Bayisa, 2020). Bacillomycin D and fengycin produced by *B. amyloliquefaciens* LYZ69 can effectively inhibit anthracnose of *Medicago sativa* (Hu et al., 2021).

In addition to the beneficial rhizosphere microorganisms that have been well investigated in their roles in the management of plant diseases (Wang et al., 2021; Zhuang et al., 2021), some lines of research indicate that phyllosphere microbial communities, namely, those of bacteria, fungi, and protozoa are also closely related to plant health as well as disease progression (Gu et al., 2010; Yang et al., 2017). The next-generation sequencing techniques are extensively applied for comprehensive analysis of the structure of microbial communities such as phyllosphere microbiome (Zhou et al., 2018; Vu et al., 2019). The sequences of 16S ribosomal RNA or the internal transcribed spacer (ITS) are currently used for amplification to analyze phyllosphere bacterial or fungal communities, respectively, (Vorholt, 2012). Recent studies indicated that the application of beneficial microorganisms, as well as microbial pesticides, can regulate the microbial community composition of the phyllosphere, thereafter promoting plant fitness and alleviating symptoms (Vorholt, 2012; Podolich et al., 2015). For example, foliar application of *B. megaterium* PB50 improved plant growth under various stress conditions by changing the structure of phyllosphere microbiota during the reproductive stage of rice (Arun et al., 2020). *B. amyloliquefaciens* B1408 was reported to promote plant growth and suppress cucumber fusarium wilt disease by changing the microbial community composition in

the rhizosphere (Han et al., 2018). Studies also showed that *Pseudomonas putida* KT2440 can drastically reduce necrosis on the leaves of *Nicotiana benthamiana* by influencing the microbial composition of the rhizosphere and phyllosphere (Bernal et al., 2017).

The yield and quality of crops are affected by many factors, among which the occurrence of diseases is usually the dominant one (Pan et al., 2021). *Alternaria alternata* is a facultative saprophytic fungus infecting over 400 species of host plants and ubiquitously causes leaf spot or leaf blight by synthesizing various kinds of mycotoxin, which pose threats to food safety and human health (Liu et al., 2020; Huang et al., 2021). Epidemiological studies also demonstrated that *A. alternata* released a large number of fungal spores in the atmosphere, making the disease hard to prevent and control (Woudenberg et al., 2015). Tobacco mosaic virus (TMV) is also a well-investigated plant virus with broad host ranges and causes significant economic losses in agriculture (Roossinck, 2015). The two pathogens above are ubiquitous and serious, causing huge losses to crop yield and agricultural economy every year (Wang et al., 2017; Chen et al., 2020). Traditional management methods, such as seedling grafting, crop rotation, and chemical strategies, have been suggested to control tobacco diseases, but these approaches are not economical, reliable, or environmentally friendly (Zhang et al., 2020).

Compared with in-depth research on the role of root colonization microbiota in plant health (Palmieri et al., 2016; Shi et al., 2016, 2017), few studies have been conducted on the potential interactions between phyllosphere microbial communities and plant diseases. In this study, the newly identified *B. velezensis* SYL-3 showed a significant inhibitory effect on *A. alternata* and TMV. In addition, a microbiome high-throughput sequencing was performed and the results suggested that SYL-3 can reduce the incidence of tobacco leaf diseases probably by promoting the phyllosphere microbial community structure, which provided a valuable theoretical basis for the biological control of tobacco diseases.

Materials and methods

Biomaterials and growth conditions

Biocontrol strain SYL-3 and *A. alternata* were isolated from tobacco leaves in Luzhou (105°26'E, 28°52'N), Sichuan Province of China, which were isolated and stored on the potato dextrose agar (PDA) and Luria–Bertani (LB) medium (Solarbio, Beijing, China) at 4°C, respectively, and were activated at 28°C for subsequent experiments. TMV virions were purified from pCB-TMV-SY (no. MG516107) inoculated *N. benthamiana* leaves according to Gooding's method and diluted to 20 µg/mL with 10 mM phosphate-buffered saline. The *Nicotiana glutinosa* and *Nicotiana tabacum* cv. NC89 plants were cultivated at the 26°C

growth chamber and were treated at the fifth to seventh leaf stage for subsequent experiments.

Bacterial identification

The strain SYL-3 was identified by Gram staining, morphology, physiological, and biochemical tests according to Bergey's Manual of Determinative Bacteriology (Brenner et al., 2005). Further identification of SYL-3 was confirmed by the analysis of 16S rRNA and *gyrA* gene sequences. Genomic DNA was isolated according to the standard phenol:chloroform procedure. The 16S rRNA gene was amplified by PCR with the bacterial universal primer pair 27F:5'-AGTTTGATCMTGGCTCAG-3' and 1492R:5'-GGTTACCTTGTACGACTT-3' (Marchesi et al., 1998). Primer pair *gyrA*-F:5'-CAGTCAGGAAATGCGTACGTCCTT-3' and *gyrA*-R:5'-CAAGGTAATGCTCCAGGCATTGCT-3' was used to amplify the partial gene sequence of *gyrA* (Yang et al., 2017; Zhang X. et al., 2017; Dhruv et al., 2020; Wu et al., 2021). The obtained PCR products were sequenced (Sangon Biotech Co., Ltd) and BLAST alignment was performed in GenBank according to sequence homology. Then, phylogenetic analysis was performed using MEGA7.0 by the neighbor-joining method with 1,000 bootstrap replications.

The colonization of the SYL-3 strain

Bacillus competent cell preparation and electrotransformation were performed according to a previous study (Wang B. et al., 2020). SYL-3 was transformed with a pGFP78 plasmid that was kindly provided by Prof. Wang Qi from China Agricultural University. The SYL-3 expressing GFP was designated as SYL-3-*gfp* and incubated in a 100 mL of LB agar medium (containing 50 µg/mL of ampicillin and tetracycline) at 28°C, 180 r/min. Then, *N. tabacum* cv. NC89 plants were treated with SYL-3-*gfp* bacterial suspension (10⁹ CFU/mL), and the colonization of SYL-3-*gfp* strain on tobacco leaves was detected based on fluorescence signal. The GFP fluorescence was photographed under ultraviolet illumination by a B-100AP longwave-UV lamp (Ultra-Violet Products, Upland, CA, United States.) and laser scanning confocal microscope (Olympus Co., Ltd, Japan, FV3000).

Effects of SYL-3 on pathogenic microorganisms

The inhibitory effect of SYL-3 against *A. alternata* was determined using *in vitro* antagonism assay as previously described (Ren et al., 2012). Briefly, a fungus plug measuring 5 mm in diameter was placed at the center of the PDA, and

1 µL of bacterial culture (10⁹ CFU/mL) was deposited on both sides of the fungus block. All tests were performed in triplicate. The plates were incubated at 28°C for 4 days, at which time the antifungal efficacy of treatments was evaluated and recorded. Leaves of *N. glutinosa* at the same position were inoculated with 100 µg TMV virions and treated with SYL-3 bacterial suspension (10⁹ CFU/mL) or ningnanmycin (An et al., 2019) at 12 h post-inoculation. Meanwhile, leaves inoculated with TMV virions (100 µg) and treated with sterile water only were served as control treatments. The local lesion numbers were recorded 3–4 days post-inoculation.

Plot test

Plot experiments with four treatments, namely, SYL-3 bacterial suspension, ningnanmycin (8% water, Deqiang Biology Co., Ltd., China), dimethachlon (40% wettable powder, Jiangxi Heyi Chemical Co., Ltd., China), and sterile water were conducted in Luzhou planting field (105°26'E, 28°52'N) using tobacco variety Yunyan No. 87. Those two pesticide treatments were served as positive control groups and water treatment was used as blank control. Each agent treated 60 tobacco plants per treatment and consisted of three biologically independent replicates. The concentration of the bacterial suspension is 10⁹ CFU/mL, and dimethachlon and ningnanmycin were diluted to 36 µg/mL and 75 µg/mL in the field experiment, respectively. Each plant was treated with about 30 mL of bacterial suspension and the leaves were sprayed evenly on both sides, at 0, 7, and 14 days, respectively.

Disease incidence estimating, sample collection, and phyllosphere microbe elution

A random sampling method was used to select five points in each plot, and four tobacco plants were selected at each point and marked to investigate the disease index on 16 June 2021 (before SYL-3 application), 23 June 2021 (7 days after SYL-3 application), 30 June 2021 (14 days after SYL-3 application), and 7 July 2021 (21 days after SYL-3 application), respectively. The degrees of disease infection (*r*) were classified into six grades (0, 1, 3, 5, 7, and 9) as previously described (Sama et al., 2019). The mean disease index of diseased tobacco plants was calculated by the following equation:

$$\text{Disease index}(\%) = \left[\frac{\sum (r \times ni)}{nt \times R} \right] \times 100$$

where *r* represents the degree of disease infection, *ni* represents the number of infected plants corresponding to the grade of *r*, *nt* represents the total number of tested plants, and *R* represents the value of the highest degree of disease infection among the

plants. The disease control rate was calculated according to the following equation:

$$\text{Disease control rate (\%)} = (C_i - T_i)/C_i \times 100$$

C_i represents the disease index of control and T_i represents the disease index of the treatments. After the fourth disease investigation, five fields were selected by random sampling method in SYL-3 bacterial suspension and blank control-treated plots. Twenty randomly selected tobacco plants and four leaves per plant were collected from each treatment group. Thereafter, 10 g of each sample was vibrated in 100 mL of sterile water at 170 r/min for 30 min and then under ultrasonic conditions for 5 min. The vibration and ultrasonic operations were repeated three times. Finally, the supernatant was transferred to 50 mL centrifuge tubes, centrifuged at 12,000 r/min for 10 min to collect the precipitated microorganisms, and quickly placed in liquid nitrogen for subsequent experiments.

DNA extraction, amplification, and sequencing of phyllosphere microbe

Total DNA of phyllosphere microbial samples was extracted from samples using the Microbial DNA Extraction Kit (UltraClean[®] Microbial DNA Kit, MoBio, United States) according to the instructions. Using the extracted DNA as a template for PCR reaction, the V3–V4 region of the bacterial 16S rRNA gene and the ITS1 region of the fungal 18S rRNA gene were amplified with respective primer pairs combined with adapter sequences and barcode sequences (The bacterial 16S rRNA primer sequences: Forward primer, 5'-AGTTTGATCMTGGCTCAG-3'; reverse primer, 5'-GGTTACCTTGTACGACTT-3'; the fungi ITS1 primer sequences: Forward primer, 5'-CTTGGTCATTTAGAGGAAGTAA-3'; reverse primer, 5'-GCTGCGTTCTTCATCGATGC-3'). The Quant-iT[™] dsDNA HS reagent (Thermo Fisher Scientific, Waltham, MA, United States) was used to quantify and pool all PCR products. High-throughput sequencing was carried out on the PacBio sequencing platform (Biomarker Technologies Co. Ltd, China). The SMRT Cell method (Jones and Kustka, 2017) was used to sequence marker genes, and then circular consensus sequencing (CCS) was filtered by UCHIME v4.2¹ software to acquire Optimization-CCS. The sequence was clustered by operational taxonomic units (USEARCH v10.0)² at a 97% similarity level, then the species composition of samples can be revealed by species annotation and richness analysis (RDP Classifier v2.2)³. Alpha diversity, Beta diversity, and significant

species difference analysis were carried out by MOTHUR (version v1.30)⁴ to discover the differences between samples. The raw reads generated by PacBio sequencing were submitted to the Sequence Read Archive database at NCBI (SRA)⁵, with the SRA BioProject accession number [PRJNA790673 (Bacterial communities 16s rRNA sequencing results)] and [PRJNA790671 (Fungal communities ITS sequencing results)].

Functional gene prediction

The PICRUSt software was used to infer the functional gene composition in the samples by comparing the species composition information obtained from the 16S sequencing data, thus analyzing the functional differences between different samples or subgroups (Parks et al., 2014). The differences and changes in the metabolic pathways of microbial community functional genes among samples of different groups were predicted through the difference analysis of the KEGG metabolic pathways (Wilkinson et al., 2017).

Statistical analysis

All data and Spearman correlation analysis were analyzed using the SPSS 20.0 program (SPSS Inc., Chicago, IL, United States), and the one-way analysis of variance with Duncan's test was used to assign significance as $P < 0.05$, using SparCC algorithm for correlation analysis. The correlation between the sample and other species at a certain taxonomic level can be achieved through Pearson's correlation network analysis. The network diagram of species correlation was generated by Python (Maucher et al., 2011). A linear discriminant analysis and effect size (LEfSe) was performed to identify microbial communities' biomarkers with statistical differences between different treatments (Segata et al., 2011).

Results

Identification and colonization of biocontrol strain SYL-3

The strain SYL-3 was identified by morphological, physiological, and biochemical tests, along with genetic homology analysis. The results showed that the colony of SYL-3 was milky white, dim, and opaque, with a bulged center and wrinkled edges (Figure 1A). SYL-3 was Gram-positive (Figure 1B) and rod-shaped (Figure 1C). Based on the

1 http://drive5.com/usearch/manual/uchime_algo.htm

2 <http://www.drive5.com/usearch/>

3 <https://sourceforge.net/projects/rdp-classifier/>

4 <http://www.mothur.org/>

5 <http://www.ncbi.nlm.nih.gov/Traces/sra>

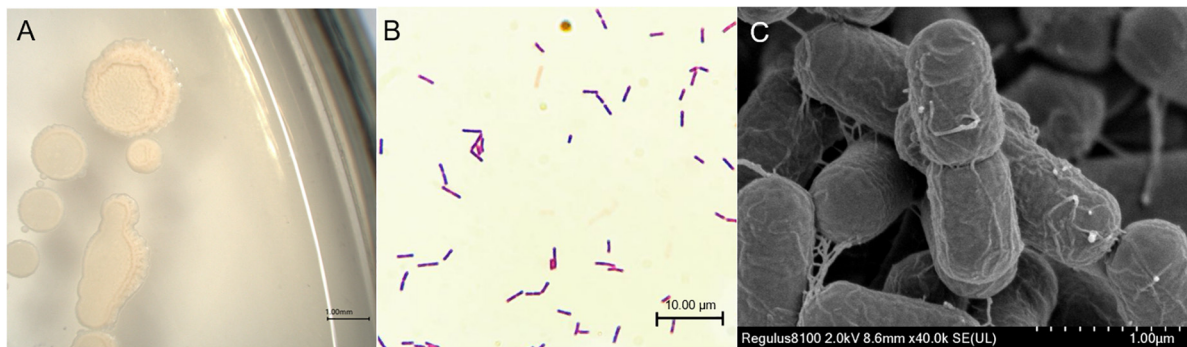


FIGURE 1

Morphological identification of SYL-3. (A) Morphology observation of SYL-3 on LB agar medium. (B) Observation of the strain SYL-3 after Gram staining. (C) Scanning electron micrographs of the strain SYL-3.

physiological and biochemical characteristics (Table 1), SYL-3 was preliminarily identified as *Bacillus* sp. Sequence alignments and phylogenetic analysis were conducted using sequences of 16S rRNA and *gyrA* gene of SYL-3. The results indicated that the 16S rRNA gene of SYL-3 was most closely related to *B. velezensis* B04 (MW418038.1), *B. velezensis* BKS104 (MW577624.1), and *B. velezensis* TB918 (CP069430.1) with 99.28, 99.10, and 99.10% sequence identity, respectively, and showed comparatively lower sequence similarity with *Bacillus safensis* U17 (CP015611.1) and *B. cellulosensis* GLB197 (CP018574.1; Figure 2A). In addition, sequencing of *gyrA* of SYL-3 showed high sequence similarity with *B. velezensis* LG37 (CP023341.1), *B. velezensis* ANSB01E (CP036518.1), and *B. velezensis* LDO2 (CP029034.1), with 99.30% sequence identity, respectively, while distantly related to *B. amyloliquefaciens* strain HM618 (CP029466.1) and *B. amyloliquefaciens* strain 9001 (KT736040.1; Figure 2B). Taken altogether, strain SYL-3 was identified as a strain of *B. velezensis*.

TABLE 1 Physiological and biochemical characteristics of SYL-3 strain.

Test index	Results (\pm)
Voges-Proskauer test	+
Citrate	-
Propionate	-
D-Xylose	+
L-Arabinose	+
D-Mannitol	+
Gelatin liquefaction	+
7%NaCl	+
PH5.7	+
Nitrate reduction	+
Starch hydrolysis	+

“+” Positive; “-” negative.

Affirming the colonization ability of biocontrol strains on host plants would lay a foundation for using the strains for disease control in the field. The GFP fluorescence expressed from SYL-3-*gfp* can be observed by fluorescence microscopy, indicating that the strain was successfully transformed with the plasmid expressing GFP (Supplementary Figure 1A). By UV light irradiation, we observed that the SYL-3-*gfp* strain evenly covered the surface of tobacco leaves 2 days after the bacterial suspension was sprayed (Supplementary Figure 1B). Furthermore, the SYL-3-*gfp* was observed around tobacco leaf epidermal cells as well as in the vascular tissue on the fourth day after treatment (Supplementary Figures 1C,D). The results confirmed the good colonization ability of SYL-3 on tobacco leaves.

SYL-3 exhibited a significant inhibitory effect against *A. alternata* and tobacco mosaic virus

To clarify the inhibitory effect of SYL-3 on *A. alternata*, we conducted an antibacterial test using *in vitro* confrontation method. The results showed that SYL-3 significantly reduced the mycelium growth of *A. alternata* by $71.33\% \pm 3.22$ (Figure 3A). To clarify the effect of SYL-3 on the infection of TMV in plants, we assessed the inhibitory activity of SYL-3 bacterial suspension against TMV by investigating the number of necrotic spots on the inoculated leaves. It showed that SYL-3 reduced the necrotic spots by $87.77\% \pm 2.81$ compared with the control treatment, suggesting a strong anti-TMV effect (Figures 3B,C).

The field plot experiments were conducted in the selected tobacco planting field with perennially occurring foliar disease caused by *A. alternata* or TMV. We thereafter used the disease index of tobacco leaves to determine the inhibitory effect of SYL-3 on these diseases. The results showed that SYL-3 significantly suppressed the disease progression of

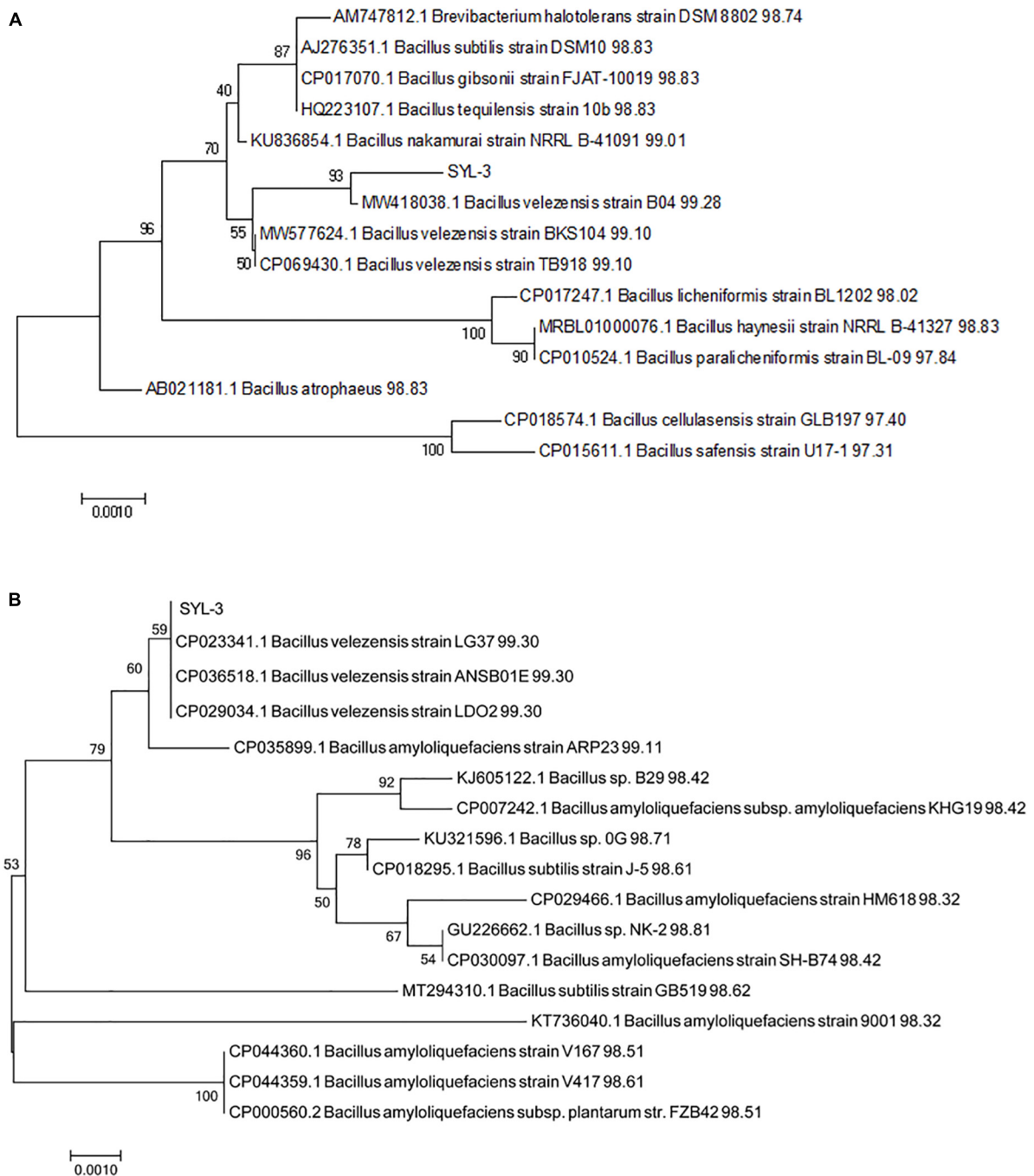


FIGURE 2

Phylogenetic analysis of strain SYL-3 based on the sequences of 16s rRNA (A) and *gyrA* (B). The tree was constructed using the neighbor-joining algorithm with 1,000 bootstrap replications.

A. alternata and reduced the respective disease index from 1.96 (control treatment) to 0.66 on day 21 after treatment (Figure 4A). Meanwhile, the disease index of *A. alternata* after dimethachlon treatment was 0.91. In addition, SYL-3 treatment also markedly suppressed mosaic leaf symptoms caused by TMV and lowered the disease index from 8.89 (control treatment)

to 2.83 (Figure 4B). In contrast, the disease index after ningnanmycin treatment was down to 4.78. The inhibitory rates of SYL-3 against *A. alternata* and TMV were determined as $50.72\% \pm 3.63$ and $68.11\% \pm 0.14$, respectively, (Figures 4C,D), which was comparatively higher than that of dimethachlon or ningnanmycin. These results collectively indicated an effective

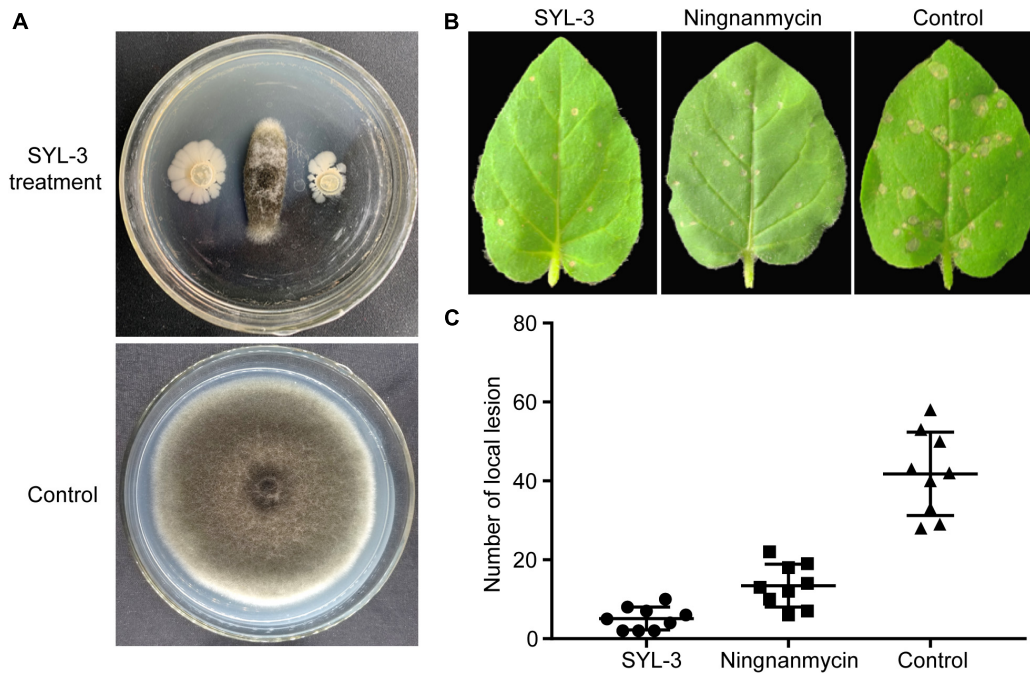


FIGURE 3
Antagonistic activities of SYL-3 against *A. alternata* and TMV. **(A)** Effects of SYL-3 on the mycelial growth of *A. alternata* *in vitro*. **(B)** Effects of SYL-3 or ningnanmycin on the necrotic lesions caused by TMV on *N. glutinosa* leaves. **(C)** Scatter plot of the necrotic lesions on *N. glutinosa* leaves treated with SYL-3, ningnanmycin, and sterile water (control).

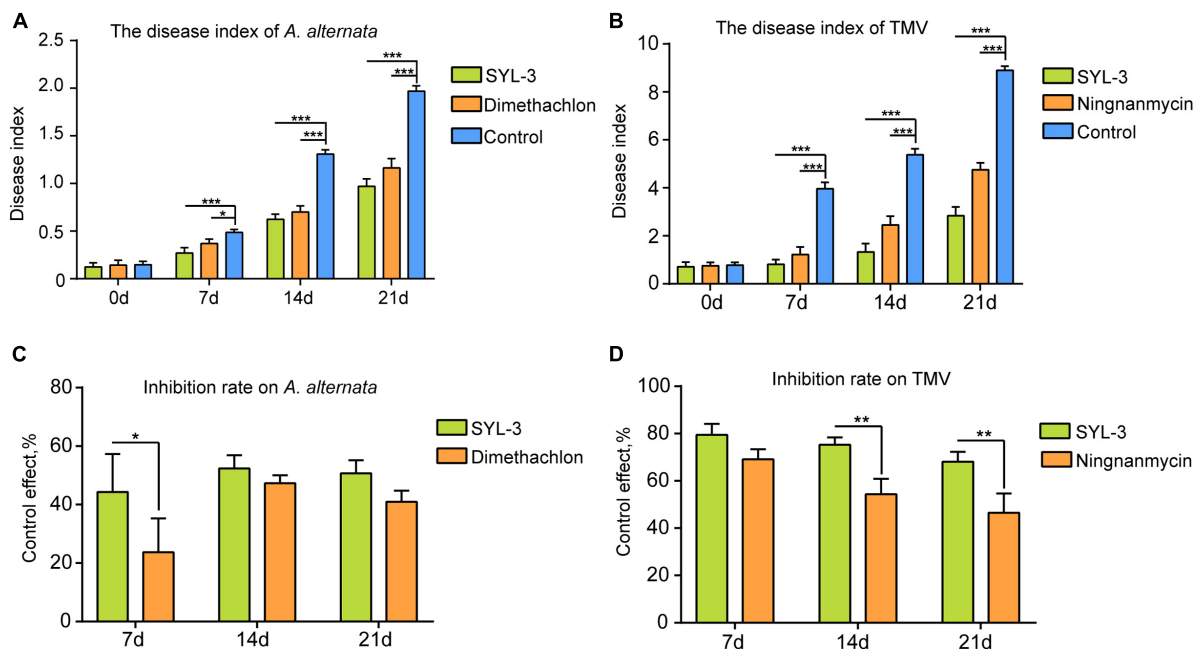


FIGURE 4
Plant disease index of *A. alternata* and TMV and control effect of SYL-3. **(A, B)** The disease index of *A. alternata* and TMV treated with SYL-3 on different days. **(C, D)** Inhibition rate on *A. alternata* and TMV treated with SYL-3 on different days (* $p < 0.05$, ** $p < 0.01$, and *** $p < 0.001$).

inhibitory effect of SYL-3 against *A. alternata* and TMV *in planta* as well as in the field.

Analysis of 16S rRNA and ITS1 sequencing data

Currently, many studies on microbial diversity are mainly based on the conserved region of nucleic acid sequences that encode ribosomal RNA as well as the ITS region (Zhuang et al., 2020). In this study, results of high-throughput sequencing analysis showed that 43,370 and 55,459 CCS were collected for SYL-3 and control treatment, respectively. A total of 38,097 and 53,599 high-quality optimization-CCS for bacteria were obtained after filtering the low-quality reads, chimeras, and attachment sequences, accounting for 88% and 97% of the total reads the number of these two treatments, respectively. Furthermore, there were 17,995 and 23,119 optimization-CCS obtained from SYL-3 and control treatment groups through ITS sequencing analysis, which accounted for about 96% and 99% of the total CCS (Table 2). The amount of sequencing data indicated that it was sufficient to reflect the species diversity in these samples.

Phyllosphere microbial community structure affected by SYL-3

The changes in the structure and composition of the phyllosphere microbial community are closely correlated with the impact of the external environment on the host plant (Vogel et al., 2020). At the genus level, we analyzed the phyllosphere microbial community structure in the control and SYL-3-treated groups on day 21 after treatment. The results showed the top 10 abundant kinds of the bacterial and fungal genus and revealed the effect of SYL-3 treatment on the phyllosphere microbial community structure of tobacco (Figures 5A,B). The abundances of *Pseudomonas*, *Sphingomonas*, and *Massilia* in the SYL-3 treatment group were increased by 19.00, 9.49, and 3.34%, respectively, compared with that of the control group (Supplementary Table 1), becoming the dominant genus of the bacterial community (Figure 5A). In contrast, the relative abundance of *Pantoea* decreased by 4.99% after SYL-3 treatment compared with the control group (Supplementary Table 1). The results of LEfSe analysis also indicated that *Pseudomonas* and *Sphingomonas* abundance were significantly increased compared with the control group (Figure 5C). Meanwhile, SYL-3 also affected the community structure of phyllosphere fungi, among which the abundance level of *Cladosporium* was markedly increased by 12.29% compared with the control group (Figures 5B,D and Supplementary Table 1). The abundance value of *Filobasidium* was also increased by 3.38%. On the contrary, the dominant fungus species *Sampaiozyma* decreased by 14.91% after SYL-3 treatment (Supplementary Table 1).

Phyllosphere microbial community diversity affected by SYL-3

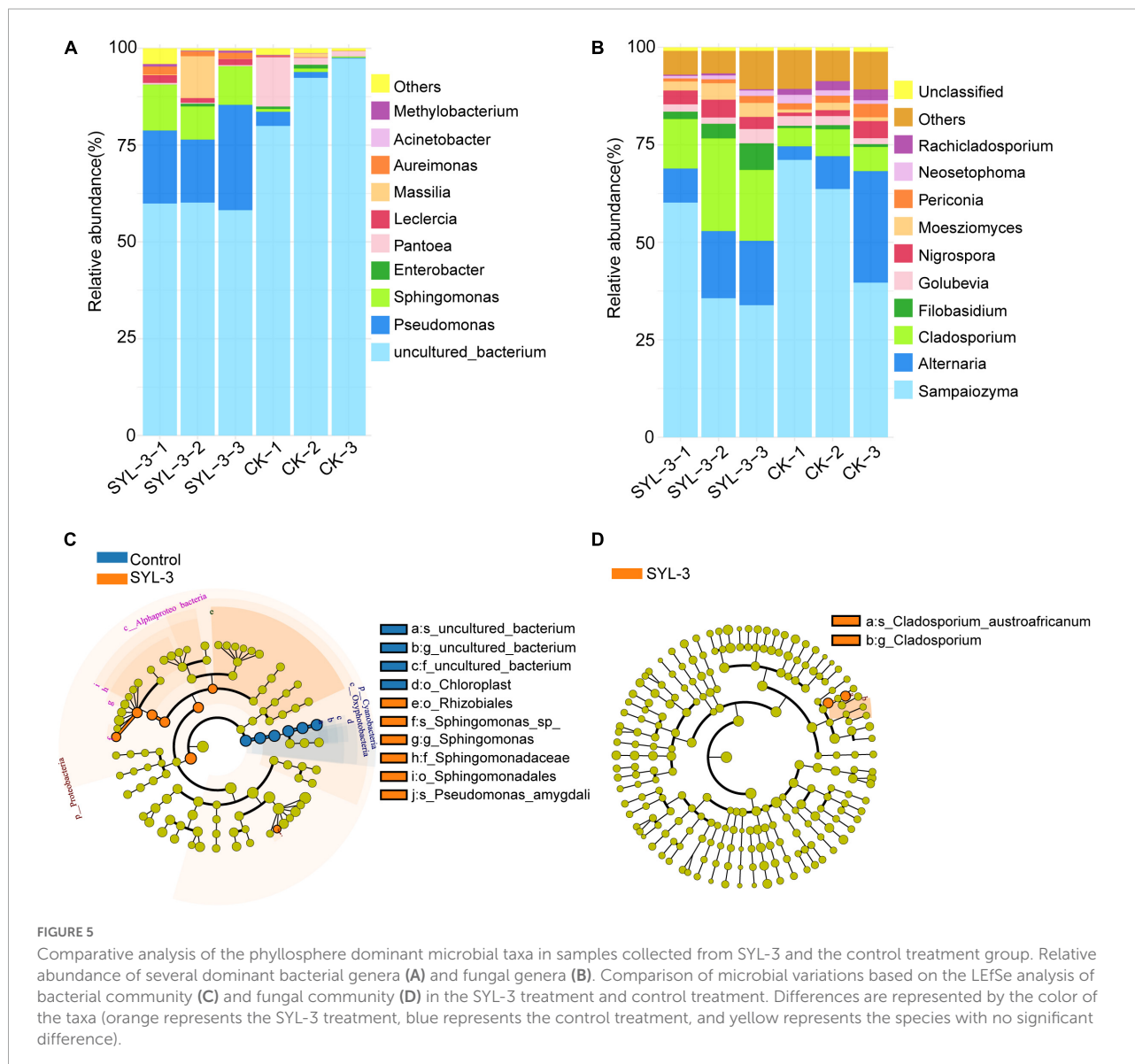
A rarefaction curve can be used to reflect the sequencing amount of microbiome samples (Wang et al., 2012). Here, the rarefaction curve of 16S rRNA and ITS1 sequencing gradually flattens out, indicating that the amount of sequencing data was sufficient to reflect the species diversity in samples (Supplementary Figure 2). In addition, to further elucidate the effects of SYL-3 on the diversity of tobacco phyllosphere microbial communities, we first analyzed the microbial community by using the diversity index. The results showed that the bacteria species richness (Chao1 and Ace index measure) and species diversity (Shannon index; Grice et al., 2009) of tobacco phyllosphere were significantly increased after SYL-3 treatment (Table 3). In contrast, the SYL-3 treatment resulted in a decrease in the Chao1 index of fungal diversity compared with that of the control treatment (Table 3). A principal coordinate analysis based on the Bray–Curtis algorithm was performed on phyllosphere microbial community samples. For fungal and bacterial communities, the spots representing the SYL-3 (red) or control (blue) treatment samples were separated (Figure 6A). In the total variance of the data set, the first two major components together comprised 94.93% and 86.77% of the total bacterial and fungal communities, respectively. In addition, the first principal component (PC1) was the most important, accounting for 86.15% and 55.77% of the total variation of bacterial (Figure 6A) and fungal communities (Figure 6B), respectively. These results revealed that phyllosphere microbial diversity significantly changed after SYL-3 treatment.

Correlation between phyllosphere microbial community structure and disease incidence

After 21 days of SYL-3 treatment, correlation analysis was performed between the abundance of dominant bacteria in tobacco phyllosphere and the disease index of common diseases. The results showed that the increase in the abundance of *Pseudomonas* and *Sphingomonas* in the phyllosphere microbes was negatively correlated ($P < 0.05$) with the disease index caused by *A. alternata* and TMV after SYL-3 treatment (Figure 7). In addition, analysis of phyllosphere microbial correlation community network showed that the relative abundance of *Pseudomonas* and *Sphingomonas* was positively correlated with the abundance of beneficial bacteria such as *Stenotrophomonas* and *Methylobacterium* (Supplementary Figure 3). Such correlation results suggested that changes in the population structure of *Pseudomonas* and *Sphingomonas* may indirectly affect the occurrence of plant diseases by SYL-3 treatment.

TABLE 2 Statistics of sample sequencing data processing result.

Treatment	16s rRNA			ITS		
	Barcode-CCS	Optimization-CCS	Effective%	Barcode-CCS	Optimization-CCS	Effective%
SYL-3	43370 ± 860.97	38097 ± 969.32	87.84 ± 3.76	18838 ± 1375.95	17995 ± 1247.74	95.53 ± 1.14
Control	55459 ± 2342.28	53599 ± 2342.65	96.65 ± 0.50	23442 ± 264.52	23119 ± 201.80	98.62 ± 0.77



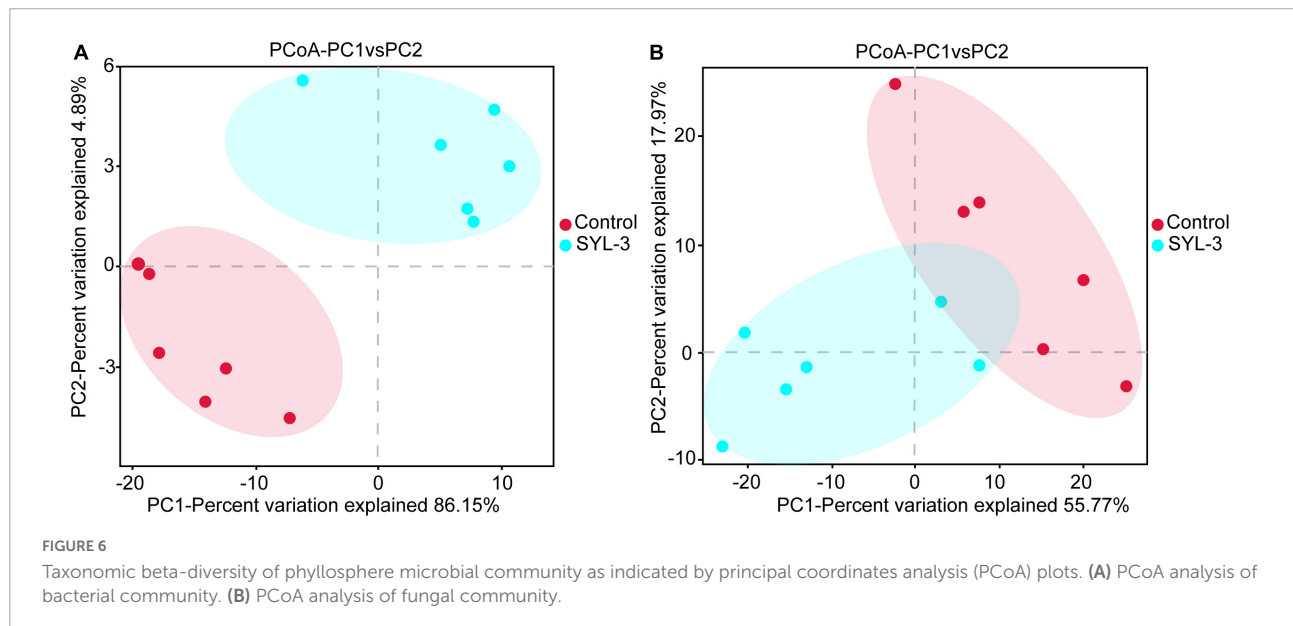
Function of tobacco phyllosphere microbial community affected by SYL-3

PICRUSt software was used to predict the composition of functional genes in the samples by comparing the species composition information obtained from the 16S

sequencing data of phyllosphere microorganisms. Then, the differences in metabolic pathways of functional genes in microbial communities between SYL-3 and control-treated samples were analyzed by KEGG (Figure 8). The KEGG metabolic pathways such as gene replication and repair, translation, nucleotide metabolism, energy metabolism, vitamin and cofactor metabolism, and the biosynthesis of other

TABLE 3 Statistics of alpha diversity index of phyllosphere microbial community.

Treatment	Community characteristics					
	Bacterial community			Fungal community		
	ACE	Chao1	Shannon	ACE	Chao1	Shannon
SYL-3	65.14 ± 3.00	65.47 ± 3.91	1.49 ± 0.13	147.26 ± 4.47	140.71 ± 4.44	2.05 ± 0.26
Control	59.22 ± 7.48	58.33 ± 8.81	0.60 ± 0.31	144.65 ± 22.66	140.94 ± 18.78	1.84 ± 0.22



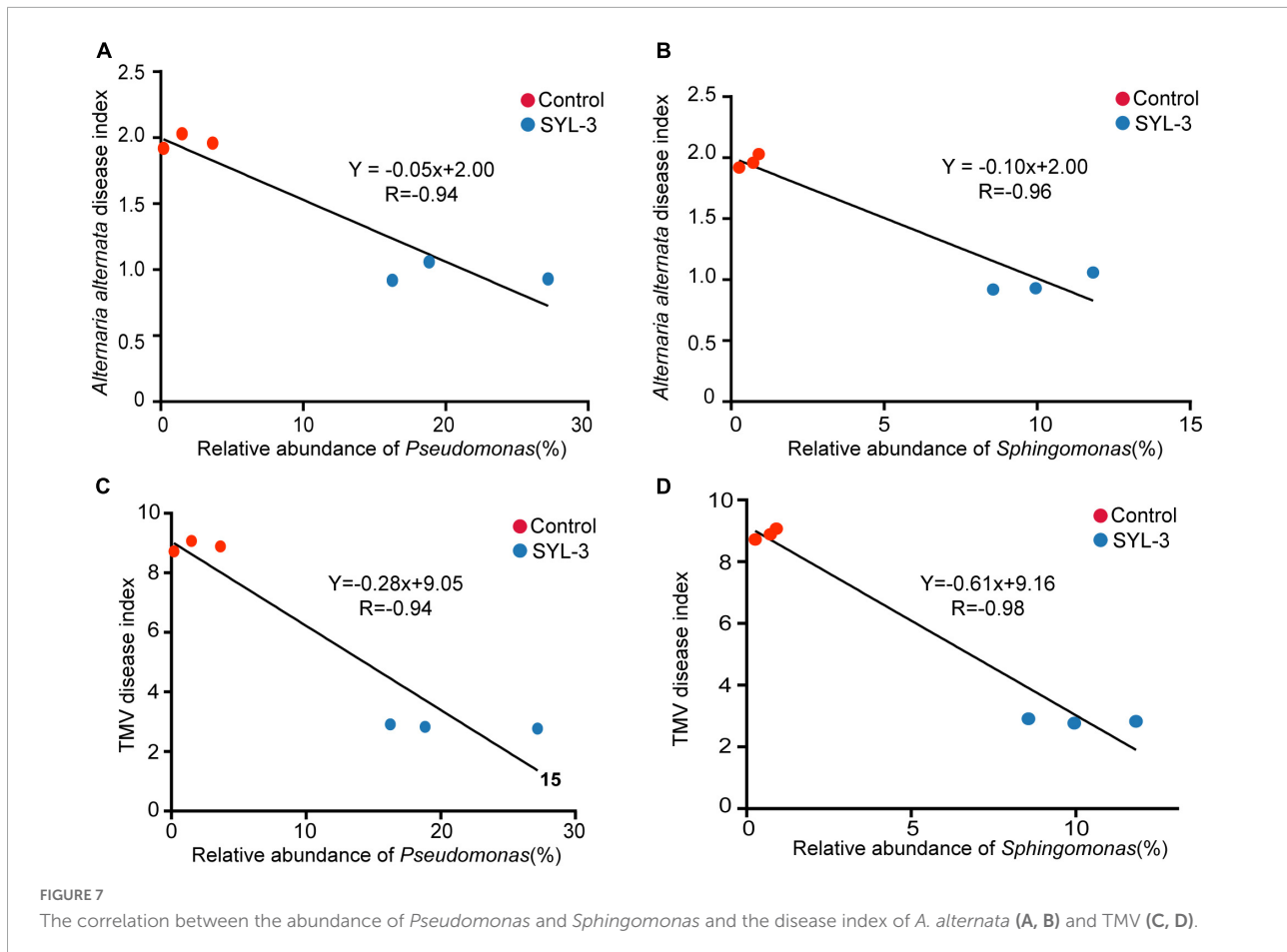
secondary metabolites were enriched after SYL-3 treatment compared with that of the control treatment. In contrast, the enrichment of pathways such as cell motility, membrane transport, and signal transduction decreased after SYL-3 treatment.

Discussion

Understanding the structure and dynamics of microbial communities is of great significance due to their effects on plant health (Gobbi et al., 2020). Previous investigations in biological control have mainly focused on soil microbial communities and revealed their critical roles in crop disease management (Palmieri et al., 2016; Shi et al., 2016, 2017). As many foliar pathogens colonize on leaf surfaces before infection, the regulation of the phyllosphere microbial community has become a new subject in biological control (Vorholt, 2012). In this study, the potential relationship among the newly isolated beneficial *B. velezensis* strain SYL-3, the phyllosphere microbial community of tobacco, and the occurrence of two ubiquitous plant diseases was investigated using microbiome high-throughput sequencing approaches.

Among the reported beneficial microorganisms and biological agents, *Bacillus* spp. has been widely applied in the management of various plant diseases (Shafi et al., 2017; Yang et al., 2020; Zhou et al., 2021). Here, phylogenetic analysis indicated that SYL-3 showed high sequence identity and clustered closely with species *B. velezensis*. Previous investigations reported that *B. velezensis* produced a variety of metabolites, regulating the microbial community structure, and can effectively inhibit a variety of crop diseases. For instance, *B. velezensis* FZB42 efficiently antagonizes *Phytophthora sojae* by producing bacilysin (Han et al., 2021). *B. velezensis* B-4 is effective in controlling *Sclerotinia sclerotiorum* by synthesizing non-ribosomal peptide synthetases, polyketide synthases, and lantipeptide synthesis proteins (Zhu et al., 2020). *B. velezensis* T052-76 can control sweet potato foot rot disease caused by *Plenodomus destruens* by altering the structure of the indigenous bacterial community (Mateus et al., 2019).

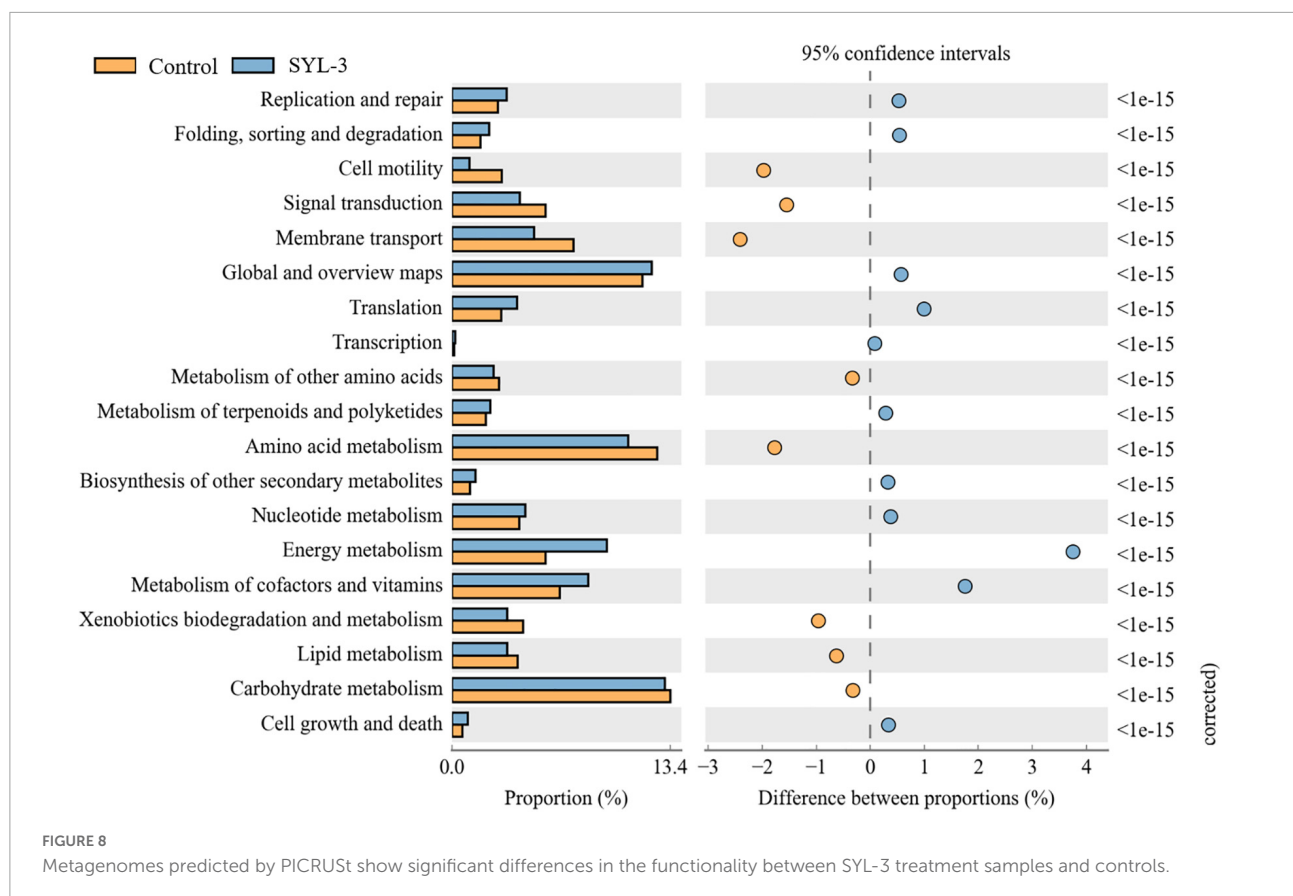
Our results showed that SYL-3 significantly affected the relative abundance of foliar bacterial communities compared with those of the fungus. Especially, the genera of *Sphingomonas* and *Pseudomonas* increased observably and became the dominant bacterial genera under SYL-3 treatment.



Sphingomonas sp. is a Gram-negative, rod-shaped aerobic bacterium that possesses multifaceted functions ranging from improving plant fitness to protecting plants from diseases (Innerebner et al., 2011; Asaf et al., 2020). The researchers demonstrated that the foliar bacterium *Sphingomonas* sp. could protect plants against the leaf-pathogenic *Pseudomonas syringae* through substrate competition (Vogel et al., 2012). The lesion coverage rate (LCR) of angular leaf spot of cucumber was correlated negatively with the abundance of *Sphingomonas* in the phyllosphere microbial community (Luo et al., 2019). *Sphingomonas* isolated from tomato leaves had strong *in vitro* antifungal activity against *B. solani*, one of the tomato pathogens (Enya et al., 2007). Herein, our research indicated that the abundance of *Sphingomonas* was negatively ($r = -0.96$) associated with *A. alternata* disease index, which was consistent with earlier reports. *Pseudomonas* sp. is a Gram-negative bacterium, which has been reported to inhibit plant diseases caused by *Ralstonia solanacearum*, *Phytophthora capsici*, and *Rhizoctonia solani* (Li, 2018; Shi, 2019), as well as induce host systemic resistance and improve morphological and biochemical traits of crops (Kumar Yadav et al., 2021). Here, the abundance of *Pseudomonas* was

negatively correlated with the TMV disease index ($r = -0.94$; Figure 7C), which is also consistent with previous reports that the *Pseudomonas* can inhibit the incidence of TMV in tomato plants and induce plant resistance (Gupta et al., 2021). Additionally, the results showed that *B. velezensis* could be detected but not as the dominant strain in the phyllosphere (Supplementary Table 1). Nevertheless, based on the good colonization capability of SYL-3, we reasonably speculate that SYL-3 treatment can exhibit a sustainable regulatory effect on phyllosphere microbial communities as well as plant pathogens.

Changes in fungal communities in the treatment groups were not as dramatic as those in bacterial communities, with only a significant increase in the abundance of *Cladosporium*. Studies have shown that *Cladosporium* produced secondary metabolites like phenylacetic acid, p-hydroxyphenyl acetic acid, and p-hydroxyphenyl ethanol, exhibiting good antibacterial and antifungal activities (Hwang et al., 2001; Kim et al., 2004; Ding et al., 2008). It has been reported that the volatile organic compounds (VOCs) produced by *Cladosporium* could promote the growth and development of tobacco as well as improve its disease resistance (Paul and Park, 2013).



Additionally, *Cladosporium* conidia can induce hypersensitive responses when in contact with tobacco leaves, activating defense responses in tobacco cells (Mattos et al., 2018). Likewise, metagenomic functional analysis of the PICRUSt predictions conducted in this study also confirmed that pathways for the biosynthesis of secondary metabolites were enriched in the treatment groups (Figure 8), which suggested that the decrease in the incidence of tobacco diseases in the treatment group may also be associated with the increase in the abundance of *Cladosporium*. Taken together, SYL-3 treatment induced the colonization of *Shingomonas*, *Pseudomonas*, *Cladosporium*, etc. in foliar microorganisms, and then the beneficial microflora above contributed to inhibiting the occurrence and progression of diseases (Figures 5, 7). However, considering which microorganism was the one playing a leading role in the disease-inhibiting event, or whether it was the result of the synergistic effect of multiple microorganisms, we still need further research on the isolation and culture of phyllosphere microorganisms.

Microbial diversity was identified as a key factor in preventing diseases and can be implemented as a biomarker in plant protection strategies (Berg et al., 2017). Several studies indicated that a relationship has been found between microbial diversity and root disease suppression. For example, traditional crop rotation reduces the outbreak potential of pathogenic

microorganisms by enhancing the overall microbial diversity in the soil (Mazzola, 2004). *B. amyloliquefaciens* FZB42, as a commercial and efficient plant strengthener, can resist *R. solani* by enhancing the overall microbial diversity (Erlacher et al., 2014). *B. subtilis* Tpb55 can effectively inhibit *Phytophthora parasitica* var. *nicotianae* by increasing bacterial diversity in tobacco rhizosphere soil (You et al., 2014). In this study, the alpha diversity of the microbial community in the SYL-3 treatment group was significantly increased, and the beta diversity of the microbial community was significantly spatially differentiated. And through the microbial correlation network analysis, it was also found that due to the increase in the diversity of phyllosphere microbes, the correlation between microbes also increased, which may lead to the formation of new homeostasis between plants and phyllosphere microbes. This is consistent with the conclusion of previous studies that greater microbial diversity has a more beneficial impact on crop resistance to pathogens (Shi et al., 2017; Han et al., 2018).

Validating the function of the microbiome is the key to revealing their relationship with the environment (Escalas et al., 2019). Inferring functions based on the diversity of bacteria at present is difficult since bacteria often transfer genes and exhibit a high degree of dependence and redundancy (Klindworth et al., 2013). Currently, PICRUSt analysis is widely explored

to acquire functional insights into the microbial community (Langille et al., 2013). This study found that several pathways that are significantly enriched after treatment, such as cofactors and vitamin metabolism pathways, are related to the promotion of plant resistance by microbial treatment (Sun et al., 2021). Studies have shown that DNA damage repair pathways mainly determine genome integrity and plant survival (Raina et al., 2021). Meanwhile, the biosynthesis of secondary metabolites of microorganisms is recognized as a rich source of biomolecules with potential medicinal applications (Li and Tan, 2017). Therefore, SYL-3 application significantly affected the function of the phyllosphere microbiome. At the same time, it indicated that SYL-3 may indirectly increase host resistance through the induction of host critical genes or pathways from the transcriptional level of some common resistance indicator genes and content of active oxygen (data not shown). Thus, it also showed the potential application value of SYL-3 as a resistance inducer for a wider range of other plant disease control.

In this study, SYL-3 belonging to *B. velezensis* was isolated and identified with a robust inhibitory effect on the infection of *A. alternata* and TMV. SYL-3 increased the abundance of several beneficial microorganisms such as *Pseudomonas*, *Sphingomonas*, and *Massilia* as well as enhanced the overall diversity of the phyllosphere microorganisms, which largely contributed to the induction of resistance against *A. alternata* or TMV. This work will improve the understanding of action modes on biocontrol for SYL-3 and provide a potential sustainable management strategy for plant diseases caused by *A. alternata* and TMV.

Data availability statement

The original contributions presented in this study are publicly available. This data can be found here: The raw reads generated by PacBio sequencing were submitted to the Sequence Read Archive database at NCBI (SRA; <http://www.ncbi.nlm.nih.gov/Traces/sra>), with the SRA BioProject accession numbers [PRJNA790673 (Bacterial communities 16s rRNA sequencing results)] and [PRJNA790671 (Fungal communities ITS sequencing results)].

Author contributions

ZW, YW, and HL conceived and designed the experiments, carried out the transcriptome analysis, and analyzed the data. HL, JJ, MA, BL, and YX performed the main experiments. HL and JJ contributed equally. CX, LJ, and HL cultivated *N. benthamiana* plants and *N. tabacum* cv. NC89 and treated samples for transcriptome sequencing. HL, MA, FY, JJ, and ZW prepared reagents, materials, and analysis tools. ZW, JJ, and HL prepared the figures and tables. HL wrote the original draft. ZW,

YW, BL, and CX reviewed drafts of the manuscript. All authors reviewed and approved the manuscript.

Funding

This research was funded by Key Scientific and Technological Projects of the Sichuan Branch of China National Tobacco Company (SCYC202113) and Key Scientific and Technological Projects of the Liaoning Branch of China National Tobacco Company (2021210000200014).

Conflict of interest

BL, YX, CX, LJ, and FY were employed by Sichuan Province Tobacco Company.

The remaining authors declare that the research was conducted in the absence of any commercial or financial relationships that could be construed as a potential conflict of interest.

Publisher's note

All claims expressed in this article are solely those of the authors and do not necessarily represent those of their affiliated organizations, or those of the publisher, the editors and the reviewers. Any product that may be evaluated in this article, or claim that may be made by its manufacturer, is not guaranteed or endorsed by the publisher.

Supplementary material

The Supplementary Material for this article can be found online at: <https://www.frontiersin.org/articles/10.3389/fmicb.2022.840318/full#supplementary-material>

SUPPLEMENTARY FIGURE 1

Colonization of SYL-3-*gfp* strain on tobacco leaves. (A) Confocal microscope observation of SYL-3-*gfp* strain. (B) UV irradiation observation of the distribution of SYL-3-*gfp* strain on the leaf surface 2 days after spraying. (C, D) Confocal microscopy observation of the colonization of SYL-3-*gfp* in leaf epidermal cells and vascular tissue.

SUPPLEMENTARY FIGURE 2

Sample rarefaction curve. (A) Rarefaction curve for bacteria in samples. (B) Rarefaction curve for fungus in samples.

SUPPLEMENTARY FIGURE 3

Pearson's correlation network analyses at genus level of phyllosphere microbial communities in SYL-3 treatment. Circles represent species, the size of the circle represents the abundance, the edges represent the correlation between the two species, the thickness of the edge represents the strength of the correlation and the color of the line: orange represents the positive correlation and green represents the negative correlation.

References

- An, M., Zhou, T., Guo, Y., Zhao, X., and Wu, Y. (2019). Molecular regulation of host defense responses mediated by biological anti-TMV agent Ningnanmycin. *Viruses* 11:815. doi: 10.3390/v11090815
- Arun, K. D., Sabarinathan, K. G., Gomathy, M., Kannan, R., and Balachandar, D. (2020). Mitigation of drought stress in rice crop with plant growth-promoting abiotic stress-tolerant rice phyllosphere bacteria. *J. Basic Microbiol.* 60, 768–786. doi: 10.1002/jobm.202000011
- Asaf, S., Numan, M., Khan, A. L., and Al-Harrasi, A. (2020). *Sphingomonas*: from diversity and genomics to functional role in environmental remediation and plant growth. *Crit. Rev. Biotechnol.* 40, 138–152. doi: 10.1080/07388551.2019.1709793
- Ashrafi, J., Rahnama, K., Babaeizad, V., Ramezanpour, S. S., and Keel, C. (2021). Induction of wheat resistance to STB by the endophytic fungus *serendipita Indica* and *Pseudomonas Protegens*. *Iran. J. Biotechnol.* 19:e2762. doi: 10.30498/IJB.2021.2762
- Bayisa, R. A. (2020). Enhancing resistance of *Sesamum indicum* against *Alternaria sesami* through *Bacillus velezensis* AR1. *Pest Manag. Sci.* 76, 3577–3586. doi: 10.1002/ps.5890
- Berg, G., Köberl, M., Rybakova, D., Müller, H., Grosch, R., and Smalla, K. (2017). Plant microbial diversity is suggested as the key to future biocontrol and health trends. *FEMS Microbiol. Ecol.* 93:fix050. doi: 10.1093/femsec/fix050
- Bernal, P., Allsopp, L. P., Filloux, A., and Llamas, M. A. (2017). The *Pseudomonas putida* T6SS is a plant warden against phytopathogens. *ISME J.* 11, 972–987. doi: 10.1038/ismej.2016.169
- Brenner, D. J., Krieg, N. R., and Staley, J. R. (2005). *Bergey's Manual of Systematic Bacteriology*. Berlin: Springer.
- Chen, Q., Cai, L., Wang, H., Cai, L., Goodwin, P., Ma, J., et al. (2020). Fungal composition and diversity of the tobacco leaf phyllosphere during curing of leaves. *Front. Microbiol.* 11:554051. doi: 10.3389/fmicb.2020.554051
- Dhruw, C., Husain, K., Kumar, V., and Sonawane, V. (2020). Novel xylanase producing *Bacillus* strain X2: molecular phylogenetic analysis and its application for production of *xylooligosaccharides*. *3 Biotech* 10:328. doi: 10.1007/s13205-020-02322-1
- Ding, L., Qin, S., Li, F., Chi, X., and Laatsch, H. (2008). Isolation, antimicrobial activity, and metabolites of fungus *Cladosporium* sp. associated with red alga *Porphyra yezoensis*. *Curr. Microbiol.* 56, 229–235. doi: 10.1007/s00284-007-9063-y
- Enya, J., Shinohara, H., Yoshida, S., Tsukiboshi, T., Negishi, H., and Suyama, K. (2007). Culturable leaf-associated bacteria on tomato plants and their potential as biological control agents. *Microb. Ecol.* 53, 524–536. doi: 10.1007/s00248-006-9085-1
- Erlacher, A., Cardinale, R., Grosch, R., Grube, M., and Berg, G. (2014). The impact of the pathogen *Rhizoctonia solani* and its beneficial counterpart *Bacillus amyloliquefaciens* on the indigenous lettuce microbiome. *Front. Microbiol.* 5:175. doi: 10.3389/fmicb.2014.00175
- Escalas, A., Hale, L., Voordeckers, J. W., Yang, Y., Firestone, M. K., Alvarez-Cohen, L., et al. (2019). Microbial functional diversity: from concepts to applications. *Ecol. Evol.* 9, 12000–12016. doi: 10.1002/ece3.5670
- Fira, D., Dimkić, I., Berić, T., Lozo, J., and Stanković, S. (2018). Biological control of plant pathogens by *Bacillus* species. *J. Biotechnol.* 285, 44–55. doi: 10.1016/j.jbiotec.2018.07.044
- Gao, L., Ma, J., Liu, Y., Huang, Y., Mohamad, O. A. A., Jiang, H., et al. (2021). Diversity and biocontrol potential of cultivable endophytic bacteria associated with halophytes from the west Aral sea basin. *Microorganisms* 9:1448. doi: 10.3390/microorganisms9071448
- Gobbi, A., Kyrkou, I., Filippi, E., Ellegaard-Jensen, L., and Hansen, L. H. (2020). Seasonal epiphytic microbial dynamics on grapevine leaves under biocontrol and copper fungicide treatments. *Sci. Rep.* 10:681. doi: 10.1038/s41598-019-56741-z
- Grice, E. A., Kong, H. H., Conlan, S., Deming, C. B., Davis, J., and Young, A. C. (2009). Topographical and temporal diversity of the human skin microbiome. *Science* 324, 1190–1192. doi: 10.1126/science.1171700
- Gu, L., Bai, Z., Jin, B., Hu, Q., Wang, H., Zhuang, G., et al. (2010). Assessing the impact of fungicide enostroburin application on bacterial community in wheat phyllosphere. *J. Environ. Sci.* 22, 134–141. doi: 10.1016/s1001-0742(09)60084-x
- Gupta, A., Verma, J., Srivastava, A., Srivastava, S., and Prasad, V. (2021). A comparison of induced antiviral resistance by the phytoalexin CAP-34 and isolate P1f of the rhizobacterium *Pseudomonas putida*. *3 Biotech* 11:509. doi: 10.1007/s13205-021-03057-3
- Han, L., Wang, Z., Li, N., Wang, Y., Feng, J., and Zhang, X. (2018). *Bacillus amyloliquefaciens* B1408 suppresses fusarium wilt in cucumber by regulating the rhizosphere microbial community. *Appl. Soil Ecol.* 136, 55–66. doi: 10.1016/j.apsoil.2018.12.011
- Han, X., Shen, D., Xiong, Q., Bao, B., Zhang, W., Dai, T., et al. (2021). The plant beneficial rhizobacterium *Bacillus velezensis* FZB42 controls the soybean pathogen *Phytophthora sojae* due to bacilysin production. *Appl. Environ. Microbiol.* 87:e0160121. doi: 10.1128/AEM.01601-21
- Hu, J., Zheng, M., Dang, S., Shi, M., Zhang, J., and Li, Y. (2021). Biocontrol potential of *Bacillus amyloliquefaciens* LYZ69 against anthracnose of alfalfa (*Medicago sativa*). *Phytopathology* 111, 1338–1348. doi: 10.1094/PHYTO-09-20-0385-R
- Huang, K., Tang, J., Zou, Y., Sun, X., Lan, J., Wang, W., et al. (2021). Whole genome sequence of *Alternaria alternata*, the causal agent of black spot of kiwifruit. *Front. Microbiol.* 12:713462. doi: 10.3389/fmicb.2021.713462
- Hwang, B., Lim, S., Kim, B., Lee, J., and Moon, S. (2001). Isolation and in vivo and in vitro antifungal activity of phenylacetic acid and sodium phenylacetate from *Streptomyces humidus*. *Appl. Environ. Microbiol.* 67, 3739–3745. doi: 10.1128/AEM.67.8.3739-3745.2001
- Innerebner, G., Knief, C., and Vorholt, J. A. (2011). Protection of *Arabidopsis thaliana* against leaf-pathogenic *Pseudomonas syringae* by *Sphingomonas* strains in a controlled model system. *Appl. Environ. Microbiol.* 77, 3202–3210. doi: 10.1128/AEM.00133-11
- Jiang, M., Xu, X., Song, J., Li, D., Han, L., Sun, X., et al. (2021). *Streptomyces botrytidirepellens* sp. nov., a novel actinomycete with antifungal activity against *Botrytis cinerea*. *Int. J. Syst. Evol. Microbiol.* 71. doi: 10.1099/ijsem.0.005004
- Jones, B. M., and Kustka, A. B. (2017). A quantitative SMRT cell sequencing method for ribosomal amplicons. *J. Microbiol. Methods* 135, 77–84. doi: 10.1016/j.mimet.2017.01.017
- Kang, B. R., Park, J. S., and Jung, W. J. (2021). Antiviral activity by lecithin-induced fengycin lipopeptides as a potent key substrate against cucumber mosaic virus. *Microb. Pathog.* 155:104910. doi: 10.1016/j.micpath.2021.104910
- Kim, Y., Cho, J., Kuk, J., Moon, J., Cho, J., and Kim, Y. (2004). Identification and antimicrobial activity of phenylacetic acid produced by *Bacillus licheniformis* isolated from fermented soybean, Chungkook-Jang. *Curr. Microbiol.* 48, 312–317. doi: 10.1007/s00284-003-4193-3
- Klindworth, A., Pruesse, E., Schweer, T., Peplies, J., Quast, C., Horn, M., et al. (2013). Evaluation of general 16S ribosomal RNA gene PCR primers for classical and next-generation sequencing-based diversity studies. *Nucleic Acids Res.* 41:e1. doi: 10.1093/nar/gks080
- Kumar Yadav, V., Krishna Jha, R., Kaushik, P., Altalayan, F. H., Al Balawi, T., and Alam, P. (2021). Traversing arbuscular mycorrhizal fungi and *Pseudomonas fluorescens* for carrot production under salinity. *Saudi J. Biol. Sci.* 28, 4217–4223. doi: 10.1016/j.sjbs.2021.06.025
- Langille, M. G., Zaneveld, J., Caporaso, J. G., McDonald, D., Knights, D., Reyes, J. A., et al. (2013). Predictive functional profiling of microbial communities using 16S rRNA marker gene sequences. *Nat. Biotechnol.* 31, 814–821. doi: 10.1038/nbt.2676
- Li, B. D. (2018). *The Study of the Control Effects of Two Biological Control Agents (Paenibacillus polymyxa and Pseudomonas fluorescens) on Tobacco Bacterial Wilt*. Master's thesis. Chongqing: Southwest University.
- Li, Y., and Tan, H. (2017). Biosynthesis and molecular regulation of secondary metabolites in microorganisms. *Sci. China Life Sci.* 60, 935–938. doi: 10.1007/s11427-017-9115-x
- Liu, H., Chen, J., Xia, Z., An, M., and Wu, Y. (2020). Effects of ϵ -poly-L-lysine on vegetative growth, pathogenicity, and gene expression of *Alternaria alternata* infecting *Nicotiana tabacum*. *Pestic. Biochem. Physiol.* 163, 147–153. doi: 10.1016/j.pestbp.2019.11.005
- Luo, L., Zhang, Z., Wang, P., Han, Y., Jin, D., Su, P., et al. (2019). Variations in phyllosphere microbial community along with the development of angular leaf-spot of cucumber. *AMB Express* 9:76. doi: 10.1186/s13568-019-0800-y
- Marchesi, J. R., Sato, T., Weightman, A. J., Martin, T. A., Fry, J. C., Hiom, S. J., et al. (1998). Design and evaluation of useful bacterium-specific PCR primers that amplify genes coding for bacterial 16S rRNA. *Appl. Environ. Microbiol.* 64, 795–799. doi: 10.1128/AEM.64.2.795-799.1998
- Mateus, J. R., Marques, J. M., Dal'Rio, I., Vollú, R. E., Coelho, M. R. R., and Seldin, L. (2019). Response of the microbial community associated with sweet

- potato (*Ipomoea batatas*) to *Bacillus safensis* and *Bacillus velezensis* strains. *Antonie Van Leeuwenhoek* 112, 501–512. doi: 10.1007/s10482-018-1181-y
- Mattos, B. B., Montebianco, C., Romanel, E., da Franca, T., Bernabé, R. B., Simas-Tosin, F., et al. (2018). A peptidogalactomannan isolated from *Cladosporium herbarium* induces defense-related genes in BY-2 tobacco cells. *Plant Physiol. Biochem.* 126, 206–216. doi: 10.1016/j.plaphy.2018.02.023
- Maucher, M., Kracher, B., Kühl, M., and Kestler, H. A. (2011). Inferring Boolean network structure via correlation. *Bioinformatics* 27, 1529–1536. doi: 10.1093/bioinformatics/btr166
- Mazzola, M. (2004). Assessment and management of soil microbial community structure for disease suppression. *Annu. Rev. Phytopathol.* 42, 35–59. doi: 10.1146/annurev.phyto.42.040803.140408
- Morelli, L., and Pellegrino, P. (2021). A critical evaluation of the factors affecting the survival and persistence of beneficial bacteria in healthy adults. *Benef. Microbes* 12, 15–25. doi: 10.1094/PHYTO-09-16-0330-RVW
- Palmieri, D., Vitullo, D., De Curtis, F., and Lima, G. (2016). A microbial consortium in the rhizosphere as a new biocontrol approach against *Fusarium* decline of chickpea. *Plant Soil* 412, 425–439. doi: 10.1007/s11104-016-3080-1
- Pan, Z., Munir, S., Li, Y., He, P., He, P., and Wu, Y. (2021). Deciphering the *Bacillus amyloliquefaciens* B9601-Y2 as a potential antagonist of tobacco leaf mildew pathogen during flue-curing. *Front. Microbiol.* 12:683365. doi: 10.3389/fmicb.2021.683365
- Parks, D. H., Tyson, G. W., Hugenholtz, P., and Beiko, R. G. (2014). STAMP: statistical analysis of taxonomic and functional profiles. *Bioinformatics* 30, 3123–3124. doi: 10.1093/bioinformatics/btu494
- Paul, D., and Park, K. (2013). Identification of volatiles produced by *Cladosporium cladosporioides* CL-1, a fungal biocontrol agent that promotes plant growth. *Sensors* 13, 13969–13977. doi: 10.3390/s131013969
- Podolich, O., Ardanov, P., Zaets, I., Pirttilä, A. M., and Kozyrovska, N. (2015). Reviving of the endophytic bacterial community as a putative mechanism of plant resistance. *Plant Soil* 388, 367–377. doi: 10.1007/s11104-014-2235-1
- Raina, A., Sahu, P. K., Laskar, R. A., Rajora, N., Sao, R., Khan, S., et al. (2021). Mechanisms of genome maintenance in plants: playing it safe with breaks and bumps. *Front. Genet.* 12:675686. doi: 10.3389/fgene.2021.675686
- Ren, X., Zhang, N., Cao, M., Wu, K., and Huang, Q. (2012). Biological control of tobacco black shank and colonization of tobacco roots by a *Paenibacillus polymyxa* strain C5. *Biol. Fertil. Soils* 48, 613–620. doi: 10.1007/s00374-011-0651-4
- Roossinck, M. J. (2015). Plants, viruses, and the environment: ecology and mutualism. *Virology* 479–480, 271–277. doi: 10.1016/j.virol.2015.03.041
- Sama, A., Mha, B., Ysm, A., Nan, B., and Ae, C. (2019). Biological control of root rot in lettuce caused by *Exserohilum rostratum* and *Fusarium oxysporum* via induction of the defense mechanism. *Biol. Control* 128, 76–84. doi: 10.1016/j.biocontrol.2018.09.014
- Sánchez-Montesinos, B., Santos, M., Moreno-Gavira, A., Marín-Rodulfo, T., Gea, F. J., and Diáñez, F. (2021). Biological control of fungal diseases by *Trichoderma aggressivum* f. *europaeum* and its compatibility with fungicides. *J. Fungi* 7:598. doi: 10.3390/jof7080598
- Segata, N., Izard, J., Waldron, L., Gevers, D., Miropolsky, L., Garrett, W. S., et al. (2011). Metagenomic biomarker discovery and explanation. *Genome Biol.* 12:R60. doi: 10.1186/gb-2011-12-6-r60
- Shafi, S., Kamili, A. N., Shah, M. A., Bandh, S. A., and Dar, R. (2017). Dynamics of bacterial class *Bacilli* in the deepest valley lake of Kashmir—the Manasbal Lake. *Microb. Pathog.* 104, 78–83. doi: 10.1016/j.micpath.2017.01.018
- Shi, L., Du, N., Shu, S., Sun, J., Li, S., and Guo, S. (2017). *Paenibacillus polymyxa* NSY50 suppresses *Fusarium* wilt in cucumbers by regulating the rhizospheric microbial community. *Sci. Rep.* 7:41234. doi: 10.1038/srep41234
- Shi, L., Du, N., Yuan, Y., Shu, S., Sun, J., and Guo, S. (2016). Vinegar residue compost as a growth substrate enhances cucumber resistance against the *Fusarium* wilt pathogen *Fusarium oxysporum* by regulating physiological and biochemical responses. *Environ. Sci. Pollut. Res. Int.* 23, 18277–18287. doi: 10.1007/s11356-016-6798-7
- Shi, M. D. (2019). *Mechanism research of Pseudomonas koreensis GS and Molecular Regulatory Mechanism of Streptomyces pactum Act12 on the Biocontrol Effect of Pseudomonas koreensis GS*. Master's thesis. Shaanxi: Northwest A&F University.
- Sun, D., Qu, J., Huang, Y., Lu, J., and Yin, L. (2021). Analysis of microbial community diversity of muscadine grape skins. *Food Res. Int.* 145:110417. doi: 10.1016/j.foodres.2021.110417
- Vogel, C., Innerebner, G., Zingg, J., Guder, J., and Vorholt, J. A. (2012). Forward genetic *in planta* screen for identification of plant-protective traits of *Sphingomonas* sp. strain Fr1 against *Pseudomonas syringae* DC3000. *Appl. Environ. Microbiol.* 78, 5529–5535. doi: 10.1128/AEM.00639-12
- Vogel, M. A., Mason, O. U., and Miller, T. E. (2020). Host and environmental determinants of microbial community structure in the marine phyllosphere. *PLoS One* 15:e0235441. doi: 10.1371/journal.pone.0235441
- Vorholt, J. A. (2012). Microbial life in the phyllosphere. *Nat. Rev. Microbiol.* 10, 828–840. doi: 10.1038/nrmicro2910
- Vu, V. H., Li, X., Wang, M., Liu, R., Zhang, G., Liu, W., et al. (2019). Dynamics of fungal community during silage fermentation of elephant grass (*Pennisetum purpureum*) produced in northern Vietnam. *Asian-Australas. J. Anim. Sci.* 32, 996–1006. doi: 10.5713/ajas.18.0708
- Wang, B., Wan, C., and Zeng, H. (2020). Colonization on cotton plants with a GFP labeled strain of *Bacillus axarquiensis*. *Curr. Microbiol.* 77, 3085–3094. doi: 10.1007/s00284-020-02071-7
- Wang, J., Wang, Y., Zhao, T., Dai, P., and Li, X. (2017). Characterization of the pathogen causing a new bacterial vein rot disease in tobacco in China. *Crop Prot.* 92, 93–98. doi: 10.1016/j.cropro.2016.10.025
- Wang, Y., Sheng, H. F., He, Y., Wu, J. Y., Jiang, Y. X., Tam, N. F., et al. (2012). Comparison of the levels of bacterial diversity in freshwater, intertidal wetland, and marine sediments by using millions of illumina tags. *Appl. Environ. Microbiol.* 78, 8264–8271. doi: 10.1128/AEM.01821-12
- Wang, Y., Zhang, C., Liang, J., Wang, L., Gao, W., Jiang, J., et al. (2020). Surfactin and fengycin B extracted from *Bacillus pumilus* W-7 provide protection against potato late blight via distinct and synergistic mechanisms. *Appl. Microbiol. Biotechnol.* 104, 7467–7481. doi: 10.1007/s00253-020-10773-y
- Wang, Z., Li, Y., Zhao, Y., Zhuang, L., Yu, Y., Wang, M., et al. (2021). A microbial consortium-based product promotes potato yield by recruiting rhizosphere bacteria involved in nitrogen and carbon metabolisms. *Microb. Biotechnol.* 14, 1961–1975. doi: 10.1111/1751-7915.13876
- Wilkinson, T. J., Cowan, A. A., Vallin, H. E., Onime, L. A., Oyama, L. B., Cameron, S. J., et al. (2017). Characterization of the microbiome along the gastrointestinal tract of growing Turkeys. *Front. Microbiol.* 8:1089. doi: 10.3389/fmicb.2017.01089
- Woudenberg, J. H., Seidl, M. F., Groenewald, J. Z., de Vries, M., Stielow, J. B., Thomma, B. P., et al. (2015). *Alternaria* section *Alternaria*: species, *formae speciales* or pathotypes? *Stud. Mycol.* 82, 1–21. doi: 10.1016/j.simyco.2015.07.001
- Wu, X., Jiang, Q., Wang, Z., Xu, Y., Chen, W., Sun, J., et al. (2021). Diversity, enzyme production and antibacterial activity of *Bacillus* strains isolated from sesame-flavored liquor Daqu. *Arch. Microbiol.* 203, 5831–5839. doi: 10.1007/s00203-021-02552-8
- Yang, F., Zhang, R., Wu, X., Xu, T., Ahmad, S., Zhang, X., et al. (2020). An endophytic strain of the genus *Bacillus* isolated from the seeds of maize (*Zea mays* L.) has antagonistic activity against maize pathogenic strains. *Microb. Pathog.* 142:104074. doi: 10.1016/j.micpath.2020.104074
- Yang, H., Li, J., Xiao, Y., Gu, Y., Liu, H., Liang, Y., et al. (2017). An integrated insight into the relationship between soil microbial community and tobacco bacterial wilt disease. *Front. Microbiol.* 8:2179. doi: 10.3389/fmicb.2017.02179
- You, C., Zhang, L. M., Ji, S. G., Gao, J. M., Zhang, C. S., and Kong, F. Y. (2014). Impact of biocontrol agent *Bacillus subtilis* on bacterial communities in tobacco rhizospheric soil. *Ying Yong Sheng Tai Xue Bao* 25, 3323–3330.
- Zeng, Y., Liu, H., Zhu, T., Han, S., and Li, S. (2021). Preparation of nanomaterial wettable powder formulations of antagonistic bacteria from *Phellodendron chinense* and the biological control of brown leaf spot disease. *Plant Pathol. J.* 37, 215–231. doi: 10.5423/PPJ.OA.02.2021.0020
- Zhang, N., Pan, R. H., Shen, Y. F., Yuan, J., Wang, L., Luo, X., et al. (2017). Development of a novel bio-organic fertilizer for plant growth promotion and suppression of rhizome rot in ginger. *Biol. Control* 114, 97–105. doi: 10.1016/j.biocontrol.2017.08.001
- Zhang, Q., Geng, Z., Li, D., and Ding, Z. (2020). Characterization and discrimination of microbial community and co-occurrence patterns in fresh and strong flavor style flue-cured tobacco leaves. *Microbiologyopen* 9:e965. doi: 10.1002/mbo3.965
- Zhang, X., Zhou, Y., Li, Y., Fu, X., and Wang, Q. (2017). Screening and characterization of endophytic *Bacillus* for biocontrol of grapevine downy mildew. *Crop Prot.* 96, 173–179. doi: 10.1016/j.cropro.2017.02.018

Zhou, L., Song, C., Muñoz, C. Y., and Kuipers, O. P. (2021). *Bacillus cabrialesii* BH5 protects tomato plants against *Botrytis cinerea* by production of specific antifungal compounds. *Front. Microbiol.* 12:707609. doi: 10.3389/fmicb.2021.707609

Zhou, L., Wang, Y., Xie, Z., Zhang, Y., Malhi, S. S., Guo, Z., et al. (2018). Effects of lily/maize intercropping on rhizosphere microbial community and yield of *Lilium davidii* var. *unicolor*. *J. Basic Microbiol.* 58, 892–901. doi: 10.1002/jobm.201800163

Zhu, Z., Peng, Q., Man, Y., Li, Z., Zhou, X., Bai, L., et al. (2020). Analysis of the antifungal properties of *Bacillus velezensis* B-4 through a bioassay and

complete-genome sequencing. *Front. Genet.* 11:703. doi: 10.3389/fgene.2020.0703

Zhuang, L., Li, Y., Wang, Z., Yu, Y., Zhang, N., Yang, C., et al. (2021). Synthetic community with six *Pseudomonas* strains screened from garlic rhizosphere microbiome promotes plant growth. *Microb. Biotechnol.* 14, 488–502. doi: 10.1111/1751-7915.13640

Zhuang, W., Yu, X., Hu, R., Luo, Z., Liu, X., Zheng, X., et al. (2020). Diversity, function and assembly of mangrove root-associated microbial communities at a continuous fine-scale. *NPJ Biofilms Microbiomes* 6:52. doi: 10.1038/s41522-020-00164-6